Interdisciplinary Research in Medical Sciences Specialty
ISSN: 3062-4401
2026, Volume 6, Issue 1, Page No: 89-98

Available online at: www.galaxypub.co/page/journals

Galaxy Publication

Near-Infrared II Fluorescence Imaging for Image-Guided Orbital Tumor Surgery: A First-in-Human Feasibility Study

James O'Leary[1]*, Aisling Dunne[1], Sean O'Brien[2]

[1]Department of Ophthalmic Oncology and Fluorescence Imaging, School of Medicine, Trinity College Dublin, Dublin, Ireland.
[2]Department of Surgical Navigation and NIR-II Imaging, School of Medicine, University College Cork, Cork, Ireland.

***E-mail** ✉ james.oleary@tcd.ie

Received: 27 November 2025; **Revised:** 27 February 2026; **Accepted:** 03 March 2026

ABSTRACT

Accurate excision of orbital tumors continues to present a major surgical challenge. Near-infrared II (NIR-II) fluorescence imaging offers surgeons the possibility of real-time visualization and localization of these tumors. This study represents the first evaluation of the feasibility and potential clinical benefit of NIR-II fluorescence imaging during orbital tumor resection. A dedicated NIR-II fluorescence imaging platform was constructed, with indocyanine green (ICG) utilized as the fluorescent contrast agent. Twenty-two patients with diagnosed orbital tumors scheduled for conventional surgery participated in the investigation. Time-dependent NIR-II imaging performed in two individuals with superficial orbital tumors established that the most suitable imaging interval was 2 h following ICG injection. In fifteen patients evaluated for diagnostic performance, both intraoperative in situ and ex vivo NIR-II fluorescence imaging demonstrated higher sensitivity and specificity than the operating surgeon's visual and tactile assessment. In the feasibility phase involving the remaining five patients, surgeons identified 34 regions of uncertainty and altered their operative plan on nine occasions based on NIR-II fluorescence guidance. Seven additional tissue resections guided by fluorescence were subsequently confirmed as appropriate by histopathological analysis, while two decisions to refrain from further excision resulted in no tumor recurrence. These outcomes support the conclusion that ICG-assisted NIR-II fluorescence imaging is a practical technique for facilitating precise resection of orbital tumors. Larger randomized controlled studies are recommended to confirm its broader clinical effectiveness.

Keywords: Fluorescence imaging, ICG, NIR-II imaging, Orbital tumor

How to Cite This Article: O'Leary J, Dunne A, O'Brien S. Near-Infrared II Fluorescence Imaging for Image-Guided Orbital Tumor Surgery: A First-in-Human Feasibility Study. Interdiscip Res Med Sci Spec. 2026;6(1):89-98. https://doi.org/10.51847/ZVcFkVdlsv

Introduction

Orbital tumors frequently compromise patients' facial aesthetics and visual acuity, making surgical removal the principal therapeutic approach. Given their intimate anatomical relationship with essential structures such as the optic nerve, extraocular muscles, and major vasculature, operative procedures must achieve complete tumor removal while safeguarding these critical tissues and maintaining satisfactory cosmetic results. Thus, the ability to perform highly precise resection is fundamental to successful orbital tumor management [1]. Over the past century, intraoperative tumor identification has largely depended on direct observation and manual palpation. In cases of diagnostic uncertainty, frozen-section histopathological examination of selected specimens has represented the definitive diagnostic method [2]. However, this technique is laborious and restricted to limited sampling, which continues to hinder the attainment of complete and accurate tumor resection [3].

A range of fluorescent agents have shown preferential uptake in neoplastic tissue, allowing tumors to become visible under appropriate excitation light. Such real-time intraoperative fluorescence imaging therefore holds considerable promise for enabling surgeons to delineate tumor boundaries across broad areas [4]. Fluorescence

imaging in the near-infrared I spectrum (NIR-I, 700–900 nm) has been the most commonly employed modality in fluorescence-guided surgery because of diminished light scattering and reduced background autofluorescence [5]. Indocyanine green (ICG), which emits in the NIR-I range, is the only fluorophore approved by the US Food and Drug Administration (FDA) for clinical near-infrared imaging applications. Clinical trials have demonstrated the diagnostic utility of ICG-based NIR-I fluorescence imaging in liver cancers [6], pancreatic tumors [7], colorectal cancer [8], meningiomas [9], and bone and soft-tissue sarcomas [10]. Nevertheless, it is not yet established whether fluorescence imaging can reliably assist precise resection of orbital tumors, which are typically approached through small incisions (<3 cm). In addition, wider implementation of fluorescence-guided surgery will require improvements in image quality and stronger evidence of clinical benefit [11].

The development of imaging within the second near-infrared window (NIR-II, 1000–1700 nm) has yielded markedly superior signal-to-noise ratios and enhanced penetration depth compared with conventional NIR-I techniques [12, 13]. Significantly, the clinically approved ICG can be effectively utilized for advanced NIR-II fluorescence imaging when paired with suitable detection systems [14]. Our earlier first-in-human investigation using a custom NIR-II imaging system and standard ICG demonstrated clear advantages for liver cancer detection, including greater tumor sensitivity, improved tumor-to-background contrast, and higher detection rates relative to NIR-I imaging [15]. Motivated by these findings, we proposed that ICG-mediated NIR-II fluorescence imaging might also enable effective identification of orbital tumors. To examine this possibility, we developed a tailored NIR-II fluorescence imaging protocol for orbital tumors employing a laboratory-built imaging apparatus. We then determined the diagnostic accuracy of this modality for orbital tumor detection and conducted an initial evaluation of its value in supporting precise surgical resection.

Materials and Methods

Study design

The present investigation incorporated both a diagnostic accuracy evaluation and a feasibility assessment, organized into three distinct phases. In the initial phase, two patients presenting with superficial orbital masses were included to optimize the NIR-II fluorescence imaging approach for orbital tumors. The second phase consisted of a prospective diagnostic study involving 15 patients diagnosed with orbital tumors. The third phase comprised a single-arm feasibility study enrolling five patients with orbital tumors to assess the impact of NIR-II fluorescence imaging on real-time surgical decisions.

These 22 individuals were recruited from the Department of Ophthalmology at the Third Medical Center of the Chinese PLA General Hospital between November 2020 and December 2022 through convenience sampling. Inclusion required patients to be 18 years of age or older, to have a confirmed clinical diagnosis of orbital solid tumors established by two senior orbital specialists, and to be scheduled for routine surgical intervention. Patients were excluded if they were younger than 18 years, had a known allergy to iodine or shellfish, or were deemed medically unfit for surgery. In addition to conventional preoperative assessments, all participants underwent gadolinium-enhanced magnetic resonance imaging (MRI) of the orbit.

NIR-II fluorescence imaging system

The custom NIR-II fluorescence imaging platform supported both open-field and closed-field operation modes. The open-field module featured a liquid-cooled InGaAs charge-coupled device (CCD) camera (Cheetah 640, Xenics) paired with a high depth-of-field lens (50 mm focal length, maximum aperture 1.8) and a 1100 nm longpass filter (FELH1100, Thorlabs). This camera was affixed to an adjustable articulated arm, enabling flexible positioning and field-of-view optimization. Fluorophore excitation was achieved using a portable 792 nm laser device (maximum output 2.0 W, Changchun Leirui Optoelectronic Technology). In the closed-field setup, both the CCD camera and laser source were positioned atop a sealed dark chamber to prevent interference from ambient light.

Preoperative time-course NIR-II fluorescence imaging for superficial orbital masses

Participants with superficial orbital masses were administered 0.7 mg kg^{-1} body weight of ICG (Dandong Yichuang Pharmaceutical, China) via intravenous infusion. Serial fluorescence images were captured with the custom NIR-II instrument at 15 min, 30 min, 1 h, 2 h, 3 h, 4 h, and 5 h after injection while patients remained in

the ward. Standard surgical resection without fluorescence guidance was performed on the subsequent day. Histopathological analysis confirmed the final diagnosis of the excised mass.

Intraoperative NIR-II fluorescence imaging for orbital tumors

Intraoperative NIR-II fluorescence imaging was applied during resection of various gadolinium-enhancing orbital tumors. Drawing on the time-course imaging data, 0.7 mg kg^{-1} body weight of ICG (Dandong Yichuang Pharmaceutical, China) was injected intravenously 2 h before the procedure. Throughout the conventional orbital surgery, in situ NIR-II imaging was conducted on the primary tumor and any additional areas where the surgeon required supplementary guidance. The tumor resection cavity was also inspected for any persistent fluorescent signals. All excised tissues underwent immediate ex vivo imaging in the closed-field NIR-II system located in the operating theater. Histopathological examination was completed for every specimen postoperatively.

Fluorescence analysis

During preoperative time-course imaging, the tumor-to-normal tissue ratio (TNR) was computed quantitatively as the ratio of average fluorescence intensity within the orbital mass to that of adjacent normal tissue. For intraoperative in situ images, three independent observers (Z.Z., L.G., and W.W.) classified regions as fluorescence-positive when they exhibited distinct hyperfluorescence relative to surrounding tissue, using a majority-vote approach. Regions were deemed fluorescence-negative if they displayed isofluorescence or hypofluorescence compared with neighboring tissue. In ex vivo assessments, TNR values were derived by comparing mean fluorescence intensity of target specimens against normal tissue from the same individual. The exploratory cutoff for optimal TNR in ex vivo imaging was established using the maximum Youden index. Fluorescence evaluators were granted access to clinical details but remained blinded to histopathological outcomes.

Histopathology assessment

Histopathological review constituted the definitive reference standard for characterizing resected tissues. Specimens were formalin-fixed, paraffin-embedded, and sectioned at 5 μm thickness. Standard hematoxylin and eosin (H&E) staining was applied to the sections. Two senior pathologists (Y.L. and Y.H.), informed of relevant clinical data but masked to NIR-II fluorescence results, independently evaluated the slides and established a consensus diagnosis.

Statistical analysis

Diagnostic judgments made by the operating surgeon, in situ fluorescence imaging, and ex vivo fluorescence imaging were benchmarked against corresponding histopathological findings. Diagnostic performance metrics—including sensitivity, specificity, receiver-operating characteristic (ROC) curves, and area under the curve (AUC) with 95% confidence intervals—were calculated to compare accuracy. Statistical computations were executed using SPSS software (version 19).

Results and Discussion

Preoperative time-course NIR-II fluorescence imaging in patients with superficial orbital masses

The initial phase aimed to establish whether NIR-II fluorescence imaging could be applied to orbital tumors and to determine the optimal interval following ICG delivery. For this purpose, two individuals with superficial orbital masses were recruited, facilitating direct, noninvasive observation over time. Prominent fluorescence appeared in a gadolinium-enhancing squamous cell carcinoma of the conjunctiva within 15 min of receiving 0.7 mg kg^{-1} body weight ICG intravenously; this diagnosis was subsequently confirmed by histopathology after removal **(Figures 1a and 1b)**. The fluorescent signal continued to be detectable without interruption for a minimum of 5 h **(Figures 1c–1h)**. Analysis of signal strength showed persistently elevated intensity during the first 2 h after injection, with a progressive reduction thereafter until 5 h **(Figure 1i)**. The tumor-to-normal tissue ratio (TNR) achieved its maximum level precisely at the 2 h time point **(Figure 1j)**. Conversely, an orbital inflammatory mass that enhanced with gadolinium exhibited no fluorescence signal despite histopathological verification. A non-enhancing epidermoid cyst likewise presented as hypofluorescent. Overall, these observations indicate that ICG-supported NIR-II imaging effectively identifies gadolinium-enhancing solid tumors while sparing inflammatory

and cystic lesions, which carries important implications for the use of fluorescence guidance in achieving accurate tumor removal.

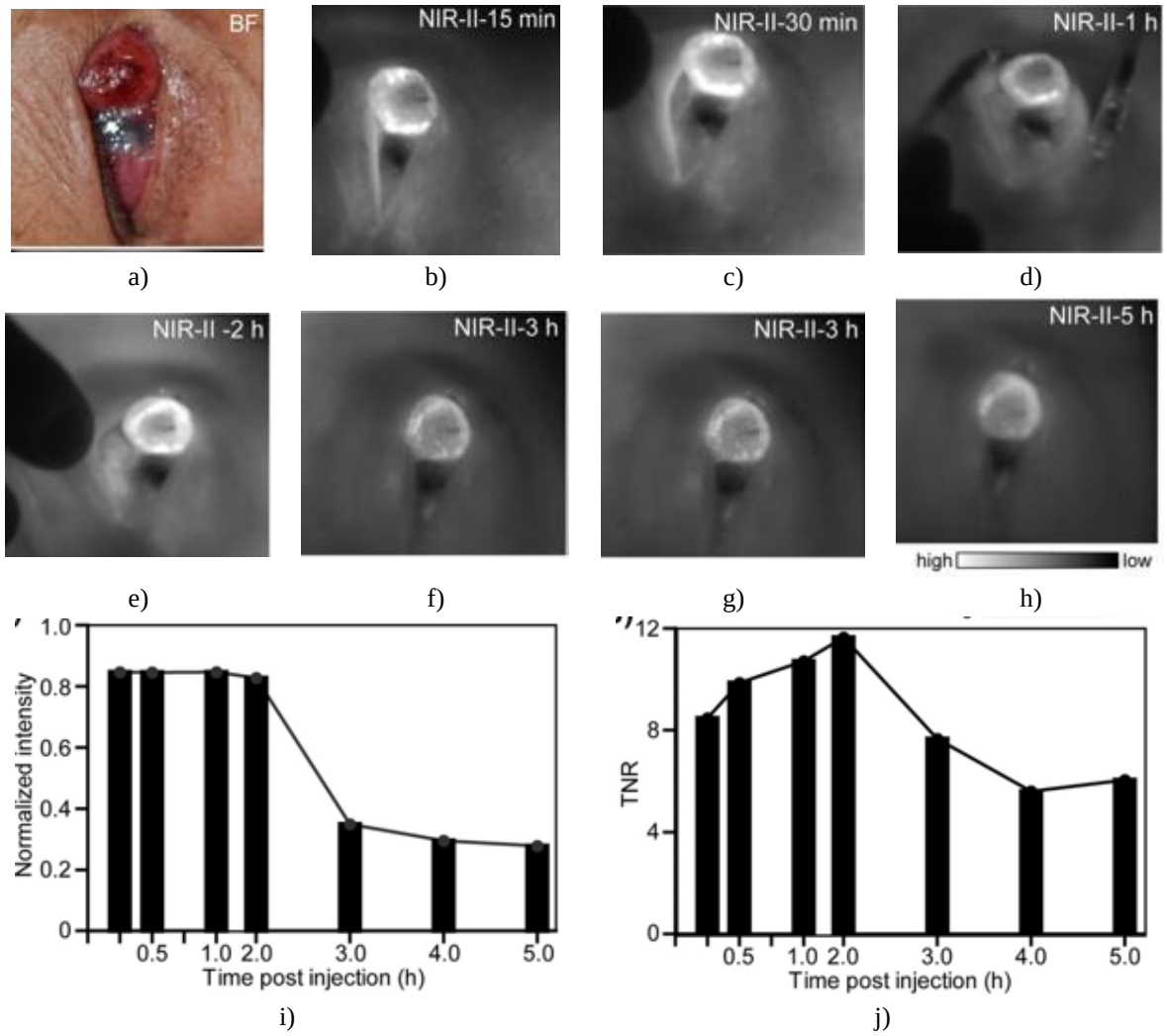

Figure 1. Time-course NIR-II fluorescence imaging conducted in patients diagnosed with squamous cell carcinoma of the conjunctiva.

(a) Bright-field photograph showing conjunctival squamous cell carcinoma. (b–h) Series of NIR-II fluorescence images recorded at progressive intervals after ICG administration. (i) Normalized fluorescence intensity levels of conjunctival squamous cell carcinoma measured at multiple time points following ICG injection. (j) Tumor-to-normal tissue ratio for conjunctival squamous cell carcinoma across different post-injection intervals with ICG. ICG, indocyanine green.

Intraoperative in situ NIR-II fluorescence imaging of orbital tumors

Given that orbital tumor excisions commonly employ limited open incisions (<3 cm), visualization remains restricted to narrow viewing angles. To overcome this constraint, researchers implemented an open-field NIR-II fluorescence imaging setup capable of dynamic adjustment of both excitation and detection orientations for improved signal optimization **(Figure 2a)**. Drawing upon the strong tumor fluorescence and maximal TNR recorded at 2 h post-injection in the conjunctival carcinoma case, 0.7 mg kg−1 body weight ICG was given intravenously to 15 patients two hours before their scheduled operations. Results demonstrated that the quality of intraoperative in situ NIR-II images depended heavily on the degree of tumor exposure. Insufficiently exposed lesions produced faint or unclear fluorescence **(Figure 2B,B')**. Once fully exposed, however, the tumors were sharply delineated in NIR-II images **(Figure 2B,C')**. Distinct fluorescence was evident in multiple tumor types during surgery, encompassing malignant examples such as orbital hemangiopericytoma and orbital malignant peripheral nerve sheath tumor, as well as benign lesions including orbital pleomorphic adenoma **(Figures 2d–2g)**.

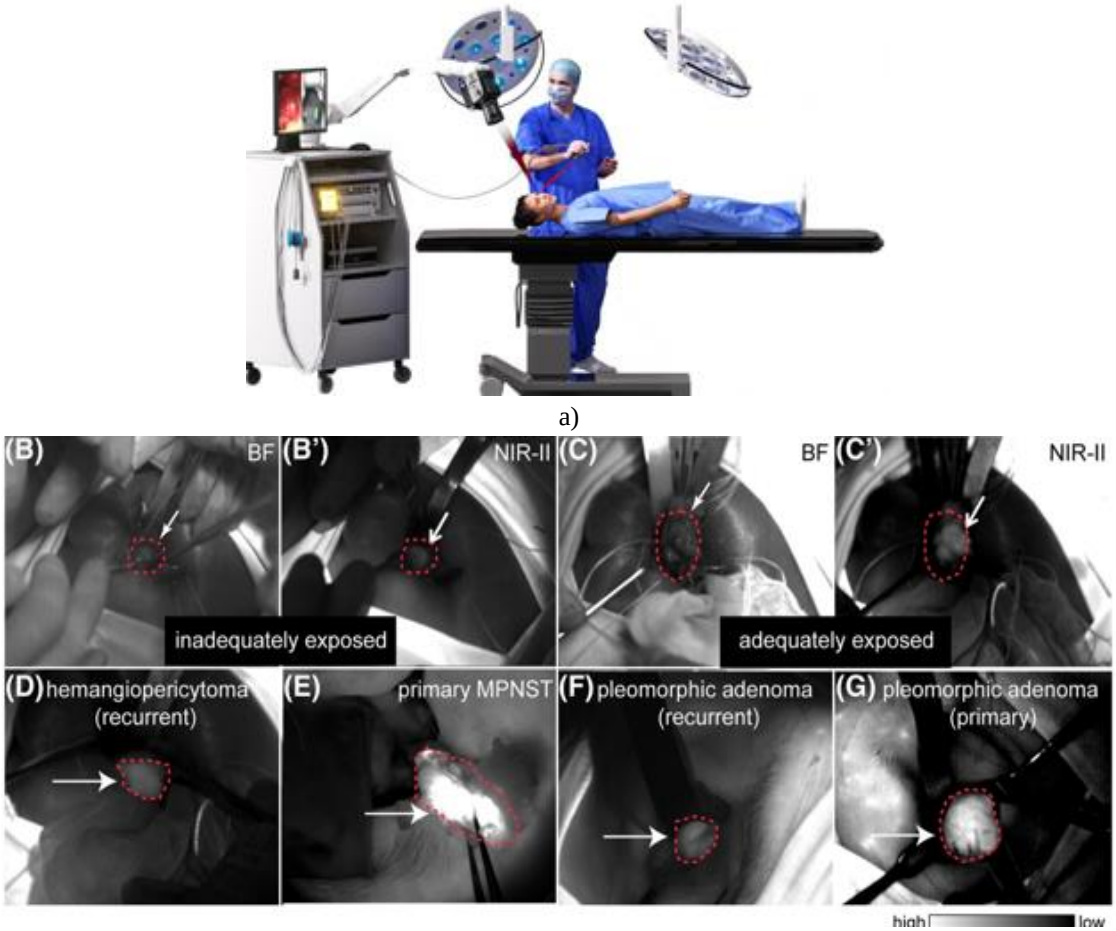

Figure 2. Intraoperative in situ NIR-II fluorescence imaging applied to patients with orbital tumors. (a) Schematic representation of the open-field NIR-II fluorescence imaging system in the surgical setting. (B and B') Bright-field photograph paired with its NIR-II fluorescence counterpart for a partially exposed orbital tumor (hemangiopericytoma). (C and C') Bright-field photograph and corresponding NIR-II fluorescence image of the identical tumor after full exposure. Red dotted circles and arrows mark the positions of the orbital tumors. (D) Intraoperative in situ NIR-II fluorescence view of the principal mass in recurrent orbital hemangiopericytoma. (E) Intraoperative in situ NIR-II fluorescence view of the principal mass in recurrent orbital malignant peripheral nerve sheath tumor. (F, G) Intraoperative in situ NIR-II fluorescence views of the principal masses in recurrent and primary orbital pleomorphic adenoma.

Subsequent evaluation focused on determining the accuracy of in situ NIR-II fluorescence imaging when applied to questionable areas during orbital tumor procedures. The surgeon initially recorded an independent impression concerning the probable presence of neoplastic tissue in each suspicious zone. These regions then received NIR-II fluorescence assessment, with classification as positive or negative based on signal strength relative to nearby unaffected tissue. Altogether, 22 adequately exposed suspicious sites, encompassing tumor resection beds and surrounding tissues, were examined intraoperatively via NIR-II imaging. Among them, 14 sites were identified as fluorescence-positive, and histopathological review verified tumor involvement in 12 of these specimens **(Figures 3a–3d)**. The other 8 sites were judged fluorescence-negative, with 5 lacking tumor cells upon pathological analysis **(Figures 3e–3h)**. When benchmarked against the surgeon's evaluations, in situ NIR-II fluorescence imaging provided improved sensitivity (80.0% versus 66.7%), specificity (71.4% versus 42.9%), and area under the curve (AUC 0.757 versus 0.548) **(Table 1)**.

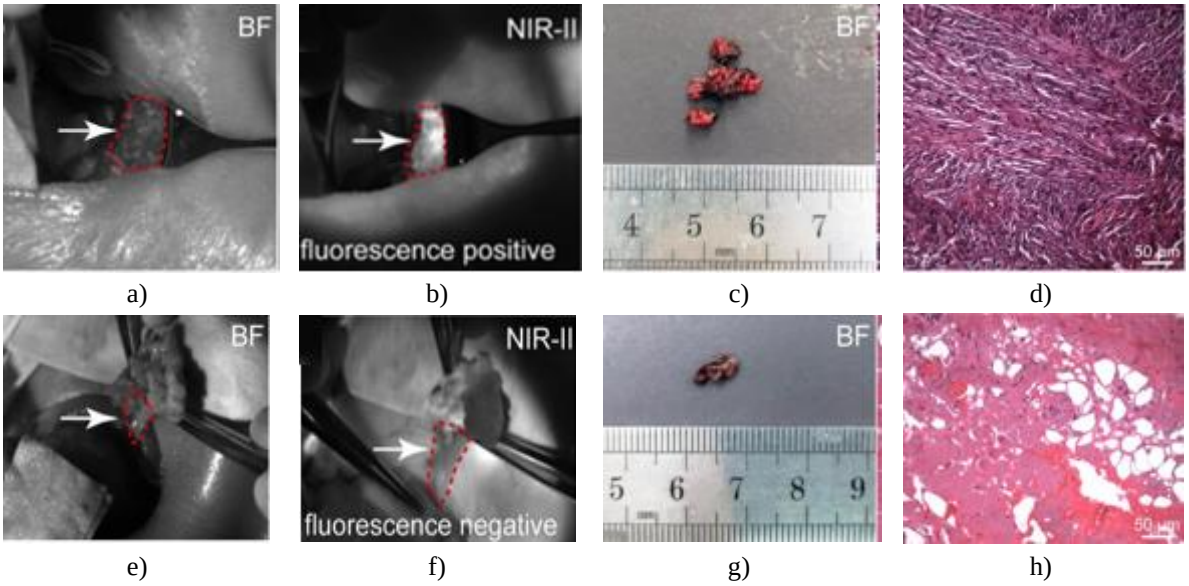

Figure 3. In situ NIR-II fluorescence imaging together with corresponding histopathological analysis of equivocal lesions.

(a, b) Bright-field photograph and associated NIR-II fluorescence image of a tumor bed captured under open-field conditions. Red dotted circles and arrows designate the specific zone where additional diagnostic support was sought by the surgeon. This zone was rated as fluorescence-positive. (c, d) Bright-field photograph and H&E-stained histological section of the excised tissue corresponding to panels A and B. Microscopic examination confirmed neoplastic cells within the specimen. (e, f) Bright-field photograph and associated NIR-II fluorescence image of adjacent para-tumor tissue under open-field conditions. Red dotted circles and arrows mark the region flagged for further evaluation by the surgeon. This region was rated as fluorescence-negative. (g, h) Bright-field photograph and H&E-stained histological section of the excised tissue corresponding to panels E and F. Microscopic examination revealed an absence of neoplastic cells. BF, bright field.

Table 1. Diagnostic performance of surgeon assessment versus NIR-II fluorescence imaging.

Reference Standard (Histopathology)	**Surgeon Assessment**		**In Situ Fluorescence Imaging**		**Ex Vivo Fluorescence Imaging**	
	Positive	**Negative**	**Positive**	**Negative**	**Positive**	**Negative**
Histopathology-confirmed positive	10	5	12	3	14	1
Histopathology-confirmed negative	4	3	2	5	1	6
Sensitivity (CI[a])	66.7% (38.7%–87.0%)		80.0% (51.4%–94.7%)		93.3% (66.0%–99.7%)	
Specificity (CI)	42.8% (11.8%–79.7%)		71.4% (30.3%–94.9%)		85.7% (42.0%–99.2%)	
AUC (CI)	0.548 (0.282–0.813)		0.757 (0.525–0.989)		0.895 (0.724–1.000)	

• a CI, confidence interval.

Diagnostic performance of in situ NIR-II fluorescence imaging for orbital tumors

The limited surgical access inherent to small incisions (<3 cm) often impedes high-resolution in situ imaging of deeply situated tumors. Therefore, an ex vivo NIR-II fluorescence strategy was adopted to better characterize excised specimens. A closed-field imaging apparatus was specifically engineered to eliminate the influence of surrounding light and standardize camera positioning **(Figure 4a)**. From the 15 patients, 86 specimens—including 26 primary tumor samples, 44 questionable para-tumor samples, and 16 normal tissue samples—were imaged ex vivo with the NIR-II system and subsequently analyzed histopathologically. Every primary tumor specimen produced intense fluorescence **(Figure 4b)**, in marked contrast to the minimal signal observed in normal orbital adipose tissue **(Figure 4c)**. Fluorescence patterns in surgeon-suspected para-tumor tissues varied considerably **(Figure 4d)**. Average fluorescence intensity was quantified and TNR values calculated using patient-matched

normal tissue as the reference. Applying histopathological diagnosis as the definitive standard, a TNR threshold of 1.21 delivered the best combined performance, attaining 92.6% sensitivity and 93.7% specificity across the full set of 86 samples. Within the 44 para-tumor specimens alone, this same threshold yielded 85.7% sensitivity and 93.7% specificity. On the 22 samples evaluated by multiple modalities, ex vivo NIR-II imaging at the 1.21 cutoff outperformed both surgeon judgment and in situ imaging, reaching 93.3% sensitivity and 85.7% specificity **(Table 1)**. Its AUC value (0.895) substantially surpassed that of the surgeon (0.548). Ex vivo NIR-II imaging also exhibited excellent correlation between fluorescence patterns and histopathological confirmation of tumor presence, along with greater TNR values than those obtained with NIR-I imaging. The complete ex vivo procedure, including quantitative assessment, was accomplished within roughly 2 min, thereby enabling timely guidance during surgery.

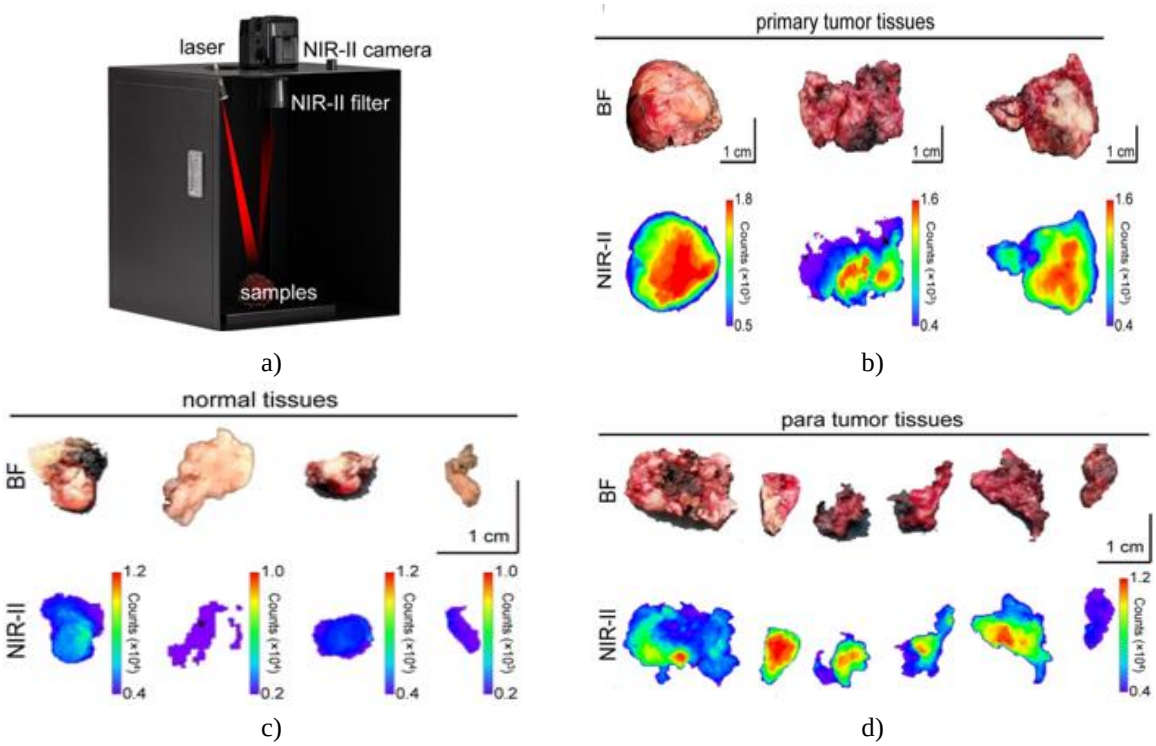

Figure 4. Closed-field ex vivo NIR-II fluorescence imaging.
(a) Diagram of the closed-field NIR-II fluorescence imaging configuration. (b–d) Representative bright-field photographs alongside corresponding NIR-II fluorescence images for primary tumor tissues, normal tissues, and para-tumor tissues.

Intraoperative ex vivo NIR-II fluorescence imaging of orbital tumors

The clinical usefulness of intraoperative NIR-II fluorescence imaging was evaluated by examining its influence on surgical decision-making during the procedure. Initially, the lead surgeon (X.Y.) relied on visual inspection and manual palpation to assess whether suspicious areas—such as the resection cavity or adjacent tissues—likely harbored residual tumor and required further excision. Intraoperative NIR-II fluorescence imaging was then performed on these regions. Based on the combined information, the lead surgeon (X.Y.) reached a definitive decision regarding tissue removal. Across five patients with orbital tumors, 34 suspicious regions were identified, all sufficiently exposed for in situ NIR-II imaging. In total, NIR-II fluorescence findings prompted a change in surgical strategy for 9 of these regions (26.5%), leading to seven additional resections and two decisions to abstain from further removal. Histopathological analysis verified the presence of tumor cells in all seven additionally excised specimens, an outcome with considerable importance for minimizing the risk of recurrence and enhancing long-term prognosis. During a mean postoperative follow-up of 31.6 months, none of the five patients showed evidence of tumor recurrence.

Safety of NIR-II fluorescence imaging

In comparison with conventional surgery, fluorescence-guided procedures involve supplementary administration of ICG and exposure to near-infrared laser light. In the current study, ICG injection was not associated with any adverse reactions. No signs of skin irritation, edema, discomfort at the irradiation site, or impairment of visual function attributable to laser exposure were observed.

Surgical management of orbital tumors is constrained by the use of small incisions, restricted tissue volumes available for removal, and the intricate surrounding anatomy. Achieving accurate and complete tumor excision in this region has remained a persistent difficulty. To the best of our knowledge, the present investigation represents the initial human study exploring NIR-II fluorescence guidance to support precision resection of orbital tumors.

It is widely recognized that ICG, functioning as a nonspecific imaging agent, tends to accumulate in various solid tumors through the enhanced permeability and retention (EPR) mechanism [16]. Moreover, prior research has identified a close association between the intensity of ICG fluorescence within tumors and the degree of gadolinium enhancement observed on preoperative MRI scans [17]. In line with these reports, the current results confirm that ICG-assisted NIR-II fluorescence imaging effectively highlights both malignant and benign gadolinium-enhancing orbital tumors. Information regarding ICG accumulation in non-neoplastic lesions, however, remains scarce. Limited clinical observations have noted that choroidal granulomas, representing a form of ocular inflammation, typically appear hypofluorescent during ICG angiography [18, 19]. In the present work, systemic delivery of ICG resulted in nonfluorescent or hypofluorescent signals from non-neoplastic masses, including inflammatory and cystic lesions. These observations strengthen the rationale for employing ICG-based fluorescence techniques to differentiate orbital tumors. Nevertheless, given the modest sample size, conclusions regarding the inability of ICG fluorescence to visualize non-neoplastic masses should be interpreted with appropriate caution.

Dynamic imaging revealed that the tumor-to-normal tissue ratio (TNR) for NIR-II fluorescence in orbital tumors reached its highest point 2 h after intravenous administration of 0.7 mg kg−1 body weight ICG. Given the short plasma half-life of ICG (approximately 2.5–3 min), this agent appears to clear rapidly from normal orbital tissues. These findings align with those of Yokoyama *et al*., who recommended an optimal imaging window of 30 min to 2 h after ICG injection for fluorescence-guided surgery of head and neck cancers, owing to enhanced tumor contrast during this period [20].

Obtaining high-quality in situ NIR-II fluorescence images of orbital tumors required adequate surgical exposure of the lesion. Beyond the imaging technology itself, the method of interpreting fluorescence signals plays a critical role in providing real-time surgical guidance. Because open-field in situ imaging is prone to interference from ambient light, surface reflectance, and variable angles—particularly within the complex orbital anatomy—objective quantitative analysis proved challenging [21, 22]. Consequently, fluorescence interpretation relied on qualitative comparison of signal intensity in target regions versus adjacent normal tissue by three independent evaluators. A comparable qualitative approach was adopted by Liberale and colleagues in ICG-based fluorescence navigation for peritoneal carcinomatosis secondary to colorectal cancer [8]. As a valuable complement to in situ imaging, the ex vivo NIR-II approach proved particularly useful for assessing poorly exposed lesions in real time. TNR values were calculated quantitatively using each patient's own normal tissue as an internal control to reduce variability arising from differences in tumor biology, tissue characteristics, injection timing, and clearance rates [23]. Earlier investigations have indicated that TNR remains relatively unaffected by ICG dosage, tumor dimensions, or histological subtype [7, 17]. Statistical optimization identified a TNR threshold of 1.21 as the most effective cutoff for classifying surgeon-suspected samples, yielding sensitivity of 92.6% and specificity of 93.7%. It should be noted, however, that this specific threshold may not be universally applicable across other tumor types. In previous work, we combined ex vivo NIR-II fluorescence imaging with artificial intelligence for intraoperative glioma identification, achieving sensitivity of 93.8% and specificity of 82.2% [24]. Nevertheless, artificial intelligence methods require large datasets, which are difficult to obtain for rare orbital tumors. Importantly, for regions where the surgeon requested additional diagnostic support, both in situ and ex vivo NIR-II fluorescence imaging outperformed conventional surgeon judgment, underscoring the potential clinical value of this modality in orbital tumor surgery.

While ICG-mediated intraoperative fluorescence imaging has demonstrated promising safety and performance in preliminary evaluations, the majority of clinical studies have concentrated on diagnostic metrics, leaving the actual patient benefit uncertain [25]. Keereweer and colleagues have proposed that the impact of fluorescence guidance on intraoperative decision-making represents the most direct and objective measure of its clinical utility [11]. In the present series, NIR-II fluorescence imaging led to modification of nine surgical decisions, with seven

additional resections subsequently confirmed to contain tumor tissue by histopathology, thereby increasing the likelihood of complete tumor removal. The two instances of conservative management showed no recurrence during follow-up. Although the rate of decision changes attributable to NIR-II imaging was 26.5%, the technique's favorable safety profile and cost-effectiveness suggest strong potential for broader adoption. Given that the participating surgeon possessed extensive experience in orbital tumor operations, ICG-based fluorescence imaging may offer even greater benefit to less experienced surgeons. These considerations support the expectation that NIR-II fluorescence guidance could enhance both oncologic and functional results. This perspective is reinforced by a pivotal randomized trial demonstrating that 5-aminolevulinic acid–guided surgery improved the extent of resection in malignant gliomas and prolonged progression-free survival [26]. More recently, Rosenthal *et al*. reported that panitumumab-IRDye800CW fluorescence imaging influenced surgical decisions in 3 of 14 patients (21.4%) [22]. Although targeted molecular probes can increase specificity, their development and clinical translation are often lengthy and resource-intensive [16, 27].

Despite providing proof-of-concept evidence for NIR-II fluorescence-guided orbital tumor surgery, several limitations of the current study warrant acknowledgment. First, the relatively small cohort of 22 patients may limit the broader applicability of the results. Second, the reliance on subjective fluorescence interpretation and convenience sampling introduces risks of selection, information, and confounding biases. Finally, the absence of a predefined TNR cutoff for fluorescence evaluation represents another constraint.

Conclusion

In summary, this study demonstrates that ICG-based NIR-II fluorescence imaging is a feasible tool for supporting precise resection of orbital tumors. Future research should prioritize the development of objective, real-time methods for fluorescence image analysis. Additionally, larger-scale investigations employing random sampling are necessary to definitively establish the clinical benefit of NIR-II fluorescence imaging in this setting.

Acknowledgments: None

Conflict of Interest: None

Financial Support: None

Ethics Statement: None

References

1. Weizman N, Horowitz G, Gil Z, Fliss DM. Surgical margins in head and neck cancer: a contemporary review. JAMA Otolaryngol Head Neck Surg. 2013;139(8):841-7.
2. Alam MS, Tongbram A, Krishnakumar S, Biswas J, Mukherjee B. Clinicopathological features and surgical outcomes of eyelid tumors: a 10-year experience. Indian J Ophthalmol. 2019;67(12):1988-93.
3. Fakurnejad S, Krishnan G, van Keulen S, Nishio N, Birkeland AC, Baik FM, et al. Intraoperative molecular imaging for head and neck cancer. Front Oncol. 2020;9:1476.
4. Liu R, Xu Y, Xu K, Dai Z. Aggregation-induced emission luminogens for bioimaging. Aggregate. 2021;2(2):e23.
5. Wu C, Gleysteen J, Teraphongphom NT, Li Y, Rosenthal E. In vivo imaging of head and neck cancer. Int J Oral Sci. 2018;10(2):10.
6. Ishizawa T, Fukushima N, Shibahara J, Masuda K, Tamura S, Aoki T, et al. Real-time identification of liver cancers by using indocyanine green fluorescent imaging. Cancer. 2009;115(11):2491-504.
7. Newton AD, Predina JD, Shin MH, Frenzel-Sulyok LG, Vollmer CM, Drebin JA, et al. Intraoperative near-infrared imaging in thoracic surgery. Ann Surg. 2019;270(1):12-20.
8. Liberale G, Vankerckhove S, Caldon MG, Ahmed B, Moreau M, Nakadi IE, et al. Fluorescence imaging for the detection of sentinel lymph nodes in breast cancer. Ann Surg. 2016;264(6):1110-6.
9. Lee JYK, Pierce JT, Thawani JP, Zeh R, Nie S, Martinez-Lage M, et al. Near-infrared fluorescence imaging for the delineation of brain tumors. J Neurosurg. 2018;128(2):380-90.

10. Nicoli F, Saleh DB, Baljer B, Chan CD, Beckingsale T, Ghosh KM, et al. Fluorescence-guided surgery for soft tissue sarcoma. Ann Surg. 2021;273(2):e63-5.
11. Lauwerends LJ, van Driel PBAA, Baatenburg de Jong RJ, Hardillo JAU, Koljenovic S, Puppels G, et al. Image-guided surgery in head and neck cancer: current practice and future directions. Lancet Oncol. 2021;22(5):e186-98.
12. Hong G, Antaris AL, Dai H. Near-infrared fluorophores for biomedical imaging. Nat Biomed Eng. 2017;1(1):0010.
13. Deng G, Zhang S, Peng X, Liu L, Tan Y, Gong P, et al. Recent advances in chemiluminescence and bioluminescence imaging. Chem Biomed Imaging. 2024. doi:10.1021/cbmi.4c00011
14. Carr JA, Franke D, Caram JR, Perkinson CF, Saif M, Askoxylakis V, et al. Shortwave infrared fluorescence imaging for cancer detection. Proc Natl Acad Sci USA. 2018;115(17):4465-70.
15. Hu Z, Fang C, Li B, Zhang Z, Cao C, Cai M, et al. First-in-human liver-tumour surgery guided by multispectral fluorescence imaging. Nat Biomed Eng. 2020;4(3):259-72.
16. Rosenthal E, Warram J, Bland K, Zinn K. The status of fluorescence-guided surgery. Ann Surg. 2015;261(1):46-56.
17. Lee JY, Thawani JP, Pierce J, Zeh R, Martinez-Lage M, Chanin M, et al. Intraoperative fluorescence imaging in neurosurgery. Neurosurgery. 2016;79(6):856-65.
18. Modi YS, Epstein A, Bhaleeya S, Harbour JW, Albini T. Intraocular lymphoma: a review. J Ophthal Inflamm Infect. 2013;3(1):58.
19. Invernizzi A, Mapelli C, Viola F, Cigada M, Cimino L, Ratiglia R, et al. Optical coherence tomography in the diagnosis of uveitis. Retina. 2015;35(3):525-30.
20. Yokoyama J, Fujimaki M, Ohba S, Anzai T, Yoshii R, Ito S, et al. Clinical significance of lymphatic spread in head and neck cancer. OncoTargets Ther. 2013;6:325-31.
21. van Keulen S, Nishio N, Fakurnejad S, van den Berg NS, Lu G, Birkeland A, et al. The clinical application of fluorescence-guided surgery in head and neck cancer. J Am Coll Surg. 2019;229(6):560-8.
22. van Keulen S, Nishio N, Fakurnejad S, Birkeland A, Martin BA, Lu G, et al. Intraoperative tumor detection using fluorescence imaging. J Nucl Med. 2019;60(6):758-65.
23. Tummers WS, Warram JM, van den Berg NS, Miller SE, Swijnenburg RJ, Vahrmeijer AL, et al. Intraoperative imaging for surgical oncology. Theranostics. 2018;8(19):5336-46.
24. Shen B, Zhang Z, Shi X, Cao C, Hu Z, Ji N, et al. Radiomics and fluorescence imaging for surgical guidance. Eur J Nucl Med Mol Imaging. 2021;48(11):3482-94.
25. Dip F, Boni L, Bouvet M, Carus T, Diana M, Falco J, et al. Consensus on fluorescence-guided surgery. Ann Surg. 2022;275(4):685-94.
26. Stummer W, Pichlmeier U, Meinel T, Wiestler OD, Zanella F, Reulen HJ. Fluorescence-guided surgery with 5-aminolevulinic acid for resection of malignant glioma. Lancet Oncol. 2006;7(5):392-401.
27. Liao Y, Peng Z, Liu X, Hu Y, Zhang J. Near-infrared fluorescence imaging in surgical oncology. Interdiscip Med. 2023;1(1):e20230024.